International Journal of Scientific Engineering and Science
Volume 8, Issue 7, pp. 50-54, 2024. ISSN (Online): 2456-7361

A Spectral Element Method for Second-order Elliptic Intersection Problem

Xuenan Zhao[1], Wei Wang[2], Jihui Zheng[3]
[1]School of Mathematical Sciences, Guizhou Normal University, Guiyang 550025, China
[2]School of Mathematical Sciences, Guizhou Normal University, Guiyang 550025, China
[3]School of Mathematical Sciences, Guizhou Normal University, Guiyang 550025, China

Abstract— *In this paper, the spectral element method for one-dimensional second-order interface elliptic problem is given. First, the corresponding Sobolev space is defined and established variational form and its discrete scheme. Secondly, the existence and uniqueness of the weak solution and its approximate solution are proved theoretically. In addition, the implementation process of the algorithm is described in detail, and a large number of numerical examples are given to prove the advantages of our algorithm. The results show that the algorithm can achieve excellent convergence and ultra-high precision for interface problems.*

Keywords— *Elliptic interface problem, spectral element method, algorithm design, numerical experiment*.

I. INTRODUCTION

The second-order elliptic interface problem is an important and fundamental problem, and many complex nonlinear problems in engineering research and scientific calculation are finally reduced to solving the second-order elliptic interface equations. Many results have been obtained in theoretical analysis and numerical calculation of second-order elliptic interface equations [1,2,3]. These numerical methods are mainly based on the finite element method [4,5] and the finite difference method [6]. In [7], Hansbo A and Hansbo P propose a non-fitting finite element method for solving elliptic interface problems based on Nitsche's method. In [8], Chen L proposed the trigonometric method of Stokes equation. In [9], Li Hong proposes a posterior error estimation method for Galerkin finite element method based on polygonal mesh.

It is well known that finite element method is flexible in the field of computation, while spectral method is a high-order numerical method with spectral accuracy [10,11]. However, there are few reports of using spectral element method to solve one-dimensional second-order elliptic interface problems. However, such numerical methods like spectral element method are of great practical significance for one-dimensional interface problems. Therefore, the aim of this paper is to find an efficient spectral element method for one-dimensional second-order elliptic interface problems. Firstly, according to the boundary conditions, proper Sobolev space is introduced to establish the weak form and discrete form of the second-order elliptic interface problem. Secondly, the Lax-Milgram lemma is used to prove the existence and uniqueness of the weak solution and the approaching solution. In addition, the construction of the basis function and the implementation of the algorithm are described in detail. Finally, a numerical example is given to verify the effectiveness and spectral accuracy of the proposed algorithm.

The rest of this article is structured as follows. In Section 2, we define a class of Sobolev spaces and establish variational forms and their corresponding discrete formats. In section 3, the existence and uniqueness of understanding is proved. In Section 4, we carefully construct the corresponding basis function in the approximation space, and the corresponding equivalent matrix form is given. In Section 5, a numerical example is given to verify the correctness of the theoretical analysis and the effectiveness of the algorithm. Finally, it is summarized in section 6.

II. WEAK FORM AND DISCRETE SCHEME

In order to better demonstrate the algorithm implementation process, we consider the following second-order elliptic interface problem:

$$\begin{aligned} &-\Delta\kappa+\alpha\kappa=\varsigma, \quad \text{in}(-1,0]\cup(0,1),\\ &\kappa(\pm1)=0, \end{aligned} \tag{1}$$

where κ is a function of x which belong to the interval $(-1,1)$, and α is a layered medium coefficient as follows:

$$\alpha=\begin{cases}1, & \text{in}(-1,0],\\ 2, & \text{in}(0,1).\end{cases}$$

Next, we establish the variational form of the equations (1) and their corresponding discrete formats. First, we introduce the following Sobolev space:

$$L^2(-1,1):=\{\kappa:\int_{-1}^{1}\kappa^2dx<\infty\},$$

$$H_*^1(-1,1):=\{\kappa:\kappa,\partial_x\kappa\in L^2(-1,1),\kappa(\pm1)=0\}.$$

The corresponding inner product definition and the norm induced by the inner product are defined as follows:

$$(\kappa,\upsilon)=\int_{-1}^{1}\kappa\upsilon dx, \quad \|\kappa\|=(\kappa,\kappa)^{\frac{1}{2}}, \tag{2}$$

$$(\kappa,\upsilon)_*=\int_{-1}^{1}\partial_x\kappa\partial_x\upsilon dx, \quad \|\kappa\|_*=(\kappa,\kappa)_*^{\frac{1}{2}}. \tag{3}$$

Then, the weak form of (1) is: Find $\kappa\in H_*^1(-1,1)$ such that

$$a(\kappa,v)=f(v), \quad \forall v\in H_*^1(-1,1), \tag{4}$$

where

$$a(\kappa,v)=\int_{-1}^{1}\partial_x\kappa\partial_x vdx+\int_{-1}^{1}\alpha\kappa vdx, \quad f(v)=\int_{-1}^{1}\varsigma vdx.$$

International Journal of Scientific Engineering and Science
Volume 8, Issue 7, pp. 50-54, 2024. ISSN (Online): 2456-7361

Note P_N as the set of all polynomials representing degree N at most. Define the approximate space V_N=$H_*^1(-1,1)\cap P_N$, then the discrete format corresponding to (4) is: Find $\kappa_N \in V_N$, such that

$$a(\kappa_N, v_N) = f(v_N), \quad \forall v_N \in V_N. \qquad (5)$$

III. Existence and Uniqueness of Solution

We use $a \lesssim b$ to represent $a \le cb$, where c is a positive constant.

Lemma 1 $\forall\ \kappa \in H_*^1(-1,1)$, *there holds*

$$\| \kappa\| \hat{} \ \| \kappa\|_*. \qquad (6)$$

Proof. According to (2), (3) and Cauchy-Schwarz inequality, it is obvious that

$$\int_{-1}^{1} \kappa^2 dx = \int_{-1}^{1} \left(\int_{-1}^{x} \partial_\tau \kappa d\tau \right)^2 dx \le \int_{-1}^{1} \left[\int_{-1}^{x} (\partial_\tau \kappa)^2 d\tau \int_{-1}^{x} 1^2 d\tau \right] dx$$

$$\hat{} \int_{-1}^{1} 1 dx \int_{-1}^{1} (\partial_\tau \kappa)^2 d\tau \hat{} \int_{-1}^{1} (\partial_x \kappa)^2 dx.$$

This finishes our proof.

Lemma 2 $a(\kappa, v)$ is a bounded and positive definite bilinear functional on $H_*^1(-1,1) \times H_*^1(-1,1)$, obviously for $\forall(\kappa, v) \in H_*^1(-1,1) \times H_*^1(-1,1)$, the following inequality holds

$$| a(\kappa, v) | \hat{} \ \| \kappa\|_* \| v\|_*, \quad a(\kappa, \kappa) \% \| \kappa\|_*^2. \quad (7)$$

Proof. From Lemma 1 and Cauchy-Schwarz inequality, we have

$$| a(\kappa, v) | = \left| \int_{-1}^{1} \partial_x \kappa \partial_x v dx + \int_{-1}^{1} \alpha \kappa v dx \right| \hat{} \ \left[\int_{-1}^{1} (\partial_x \kappa)^2 dx \right]^{\frac{1}{2}} \left[\int_{-1}^{1} (\partial_x v)^2 dx \right]^{\frac{1}{2}}$$

$$+ \left(\int_{-1}^{1} \kappa^2 dx \right)^{\frac{1}{2}} \left(\int_{-1}^{1} v^2 dx \right)^{\frac{1}{2}} \hat{} \ \| \kappa\|_* \| v\|_*.$$

In addition, we derive that

$$a(\kappa, \kappa) = \int_{-1}^{1} (\partial_x \kappa)^2 dx + \int_{-1}^{1} \alpha \kappa^2 dx \% \| \kappa\|_*^2,$$

there is no doubt that the proof is completed.

Lemma 3 If $f \in L^2(-1,1)$, $f(v)$ is a continuous linear function on $H_*^1(-1,1)$, i.e.

$$| f(v) | \hat{} \ \| v\|_*. \qquad (8)$$

Proof. From Lemma 1 and Cauchy-Schwarz inequality, we have

$$| f(v) | = \left| \int_{-1}^{1} \varsigma v dx \right| \le \| \varsigma\| \ \| v\| \hat{} \ \| v\| \hat{} \ \| v\|_*.$$

Then, based on lemmas 2-3 and the Lax-Milgram theorem, we get the following theorem 1:

Theorem 1 If $f \in L^2(-1,1)$, equations (4) and (5) exist unique solutions κ and κ_N, respectively.

IV. Design And Implementation Of the Algorithm

In this section, we shall describe how to efficiently solve (5). We start by constructing a set of basis functions of the approximation space V_N.

Let

$$\varphi_i(t) = L_i(t) - L_{i+2}(t), (i = 0,1,\cdots, N-2),$$

where $L_i(t)$ is a Legendre polynomial of degree i.

Set

$$\begin{cases} t_1 = 2x+1, \hat{\kappa}(t_1) = \kappa(x), \ \hat{f}(t_1) = \varsigma(x), x \in (-1,0), \\ t_2 = 2x-1, \hat{\kappa}(t_2) = \kappa(x), \ \hat{f}(t_2) = \varsigma(x), x \in (0,1). \end{cases}$$

We define the following internal basis functions:

$$\phi_{1,i}(x) = \begin{cases} \varphi_i(t_1(x)), & x \in (-1,0), \\ 0, & x \in (0,1), \end{cases} \quad \phi_{2,i}(x) = \begin{cases} 0, & x \in (-1,0), \\ \varphi_i(t_2(x)), & x \in (0,1), \end{cases}$$

where $i = 0,1,\cdots, N-2$. Define the basis function at the interface:

$$\phi_{N-1}(x) = \begin{cases} \varphi_{N-1,1} = \dfrac{1+t_1(x)}{2}, x \in (-1,0), \\ \varphi_{N-1,2} = \dfrac{1-t_2(x)}{2}, x \in (0,1). \end{cases}$$

Set the R_Γ is the interface, the graph of the various basis functions and their derivatives for x is as follows:

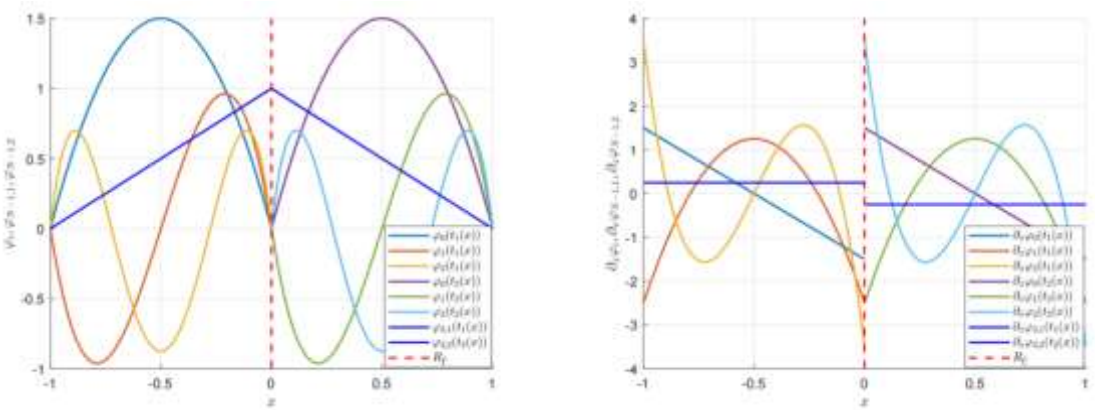

Fig. 1. The figures of the basis functions of x (left) and the derivatives of the basis functions (right) with N=4 and i=0,1,2.

It is obvious that

$$V_N = \bigcup_{j=1,2} \text{span}\left\{ \phi_{j,0}, \phi_{j,1}, \cdots, \phi_{j,N-2} \right\} \oplus \text{span}\left\{ \phi_{N-1} \right\}.$$

We expand κ_N as follows:

International Journal of Scientific Engineering and Science
Volume 8, Issue 7, pp. 50-54, 2024. ISSN (Online): 2456-7361

$$\kappa_N = \hat{\kappa}_{N-1}\phi_{N-1} + \sum_{i=0}^{N-2}\hat{\kappa}_{i,1}\phi_{1,i} + \sum_{i=0}^{N-2}\hat{\kappa}_{i,2}\phi_{2,i}. \quad (9)$$

Substitute (9) into (5) to calculate, and let V_N go through a set of basis functions in V_N, then (5) can be reduced to the following matrix form:

$$\begin{bmatrix} A_1+C_1 & \mathbf{0} & (B_1+D)^T \\ \mathbf{0} & A_2+2C_2 & (-B_2+E)^T \\ B_1+D & -B_2+E & g_0 \end{bmatrix}\begin{bmatrix} U_1 \\ U_2 \\ \hat{\kappa}_{N-1} \end{bmatrix} = \begin{bmatrix} F_1 \\ F_2 \\ f_0 \end{bmatrix}$$

where

$A_1=(a_{ji}^1), B_1=(b_i^1), C_1=(c_{ji}^1), D=(d_i), A_2=(a_{ji}^2),$

$B_2=(b_i^2), C_2=(c_{ji}^2), E=(e_i), U_1=(\hat{\kappa}_{0,1},\cdots,\hat{\kappa}_{N-2,1})^T,$

$U_2=(\hat{\kappa}_{0,2},\cdots,\hat{\kappa}_{N-2,2})^T, F_1=(f_{0,1},\cdots,f_{N-2,1})^T, F_2=(f_{0,2},\cdots,f_{N-2,2})^T,$

and

$$a_{ji}^1 = 2\int_{-1}^1 \partial_{t_1}\phi_{1,i}\partial_{t_1}\phi_{1,j}dt_1, b_j^1 = \int_{-1}^1 \partial_{t_1}\phi_{1,j}dt_1, c_{ji}^1 = \frac{1}{2}\int_{-1}^1 \phi_{1,i}\phi_{1,j}dt_1,$$

$$a_{ji}^2 = 2\int_{-1}^1 \partial_{t_2}\phi_{2,i}\partial_{t_2}\phi_{2,j}dt_2, b_j^2 = \int_{-1}^1 \partial_{t_2}\phi_{2,j}dt_2, c_{ji}^2 = \frac{1}{2}\int_{-1}^1 \phi_{2,i}\phi_{2,j}dt_2,$$

$$d_j = \frac{1}{2}\int_{-1}^1 \varphi_{N-1,1}\phi_{1,j}dt_1, e_j = \int_{-1}^1 \varphi_{N-1,2}\phi_{2,j}dt_2, f_{j,1} = \frac{1}{2}\int_{-1}^1 \hat{f}(t_1)\phi_{1,j}dt_1,$$

$$f_{j,2} = \frac{1}{2}\int_{-1}^1 \hat{f}(t_2)\phi_{2,j}dt_2, f_0 = \frac{1}{2}\int_{-1}^1 \hat{f}(t_1)\varphi_{N-1,1}dt_1 + \frac{1}{2}\int_{-1}^1 \hat{f}(t_2)\varphi_{N-1,2}dt_2,$$

$$g_0 = 2\int_{-1}^1 [\partial_{t_1}\varphi_{N-1,1}]^2 dt_1 + 2\int_{-1}^1 [\partial_{t_2}\varphi_{N-1,2}]^2 dt_2 + \frac{1}{2}\int_{-1}^1 \varphi_{N-1,1}^2 dt_1 + \int_{-1}^1 \varphi_{N-1,2}^2 dt_2,$$

where $i, j = 0,1,\cdots,N-2.$

V. Numerical Experiment

To demonstrate the convergence and superior accuracy of our algorithm, we will conduct a series of numerical tests in this section. The problem (1) are computed by using the spectral element method with different N. Our programs are compiled and operated in MATLAB R2023b.

Let $\kappa_N(x)$ be the approximate solution of $\kappa(x)$. The error between the exact solution and the approximate solution is defined as follows:

$$e(\kappa,\kappa_N) = \| \kappa(x) - \kappa_N(x) \|_{L^\infty(-1,1)}.$$

Example 1: In the case of $\kappa(x) = cos\frac{\pi x}{2}e^{(\frac{x}{2})^2}$, which obviously satisfy (1). And then we can get $\varsigma(x)$ from (1). When $N = 50$, the exact solution, the numerical solution and the error diagram are shown in Fig. 2. Table 1 lists the errors for different N.

It can be observed from Table 1 that when $N > 30$, the approximate solution has an accuracy of about 10^{-15}. In addition, Fig. 2 shows once again that our algorithm is stable and highly accurate.

Example 2: We set $\kappa(x) = \sin[\frac{\pi(1+x)}{2}]e^{2x}$. Then we can acquire $\varsigma(x)$ from (1). The exact solution, the numerical solution and the error figure between them are presented in Fig. 3. The errors $e(\kappa,\kappa_N)$ for different N are listed in Table 2.

Likewise, it can be observed from Table 2 that when $N > 40$, the approximate solution has an accuracy of about 10^{-15}. In addition, Fig. 3 shows once again that our algorithm is stable and highly accurate

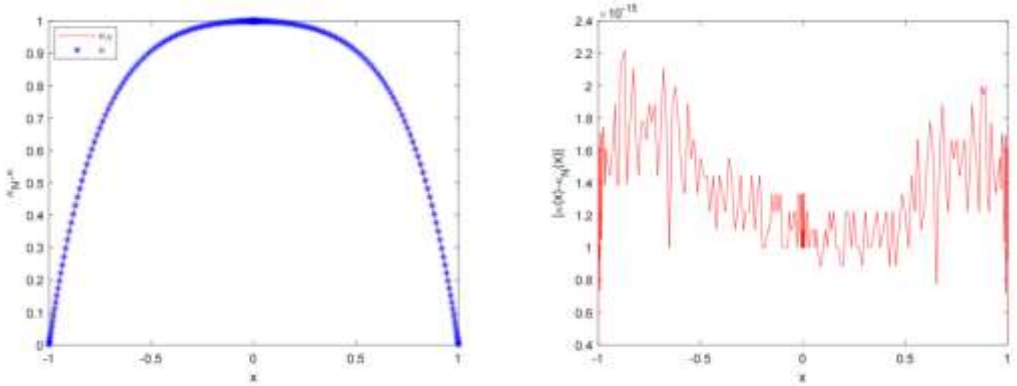

Fig. 2. Figures of the exact solution and the numerical solution with N=50 (left) and the error between them(right).

TABLE 1. The error between the numerical solution and the exact solution with different N.

	N=20	N=30	N=40
$e(\kappa,\kappa_N)$	1.75345849e-14	6.31439345e-15	3.49720253e-15
	N=50	N=60	N=70
$e(\kappa,\kappa_N)$	2.22044605e-15	1.50877574e-15	1.79804088e-15

International Journal of Scientific Engineering and Science
Volume 8, Issue 7, pp. 50-54, 2024. ISSN (Online): 2456-7361

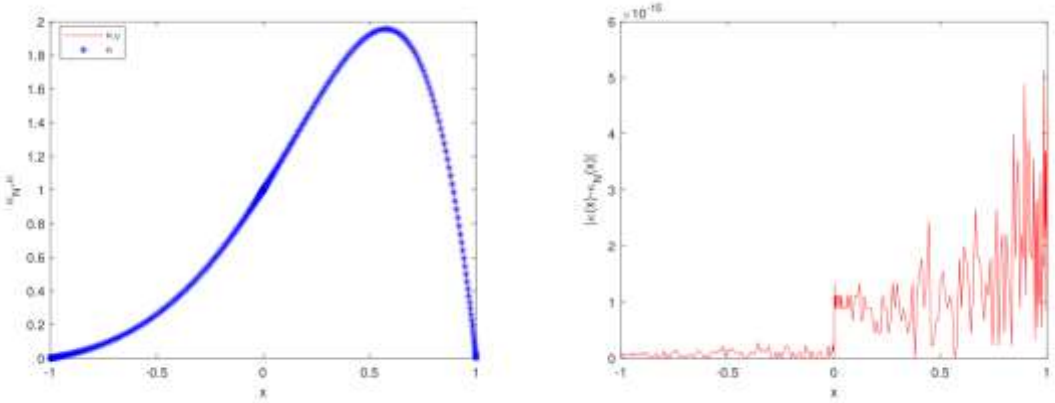

Fig. 3. Figures of the exact solution and the numerical solution with N=70 (left) and the error between them(right).

TABLE 2. The error between the numerical solution and the exact solution with different N.

	N=20	N=30	N=40
$e(\kappa,\kappa_N)$	4.70595785e-14	1.65423231e-14	9.99200722e-15
	N=50	N=60	N=70
$e(\kappa,\kappa_N)$	5.77315973e-15	4.21884749e-15	5.13478149e-15

Example 3: We take $\kappa(x) = cos\frac{\pi x}{2}\sin[\frac{\pi(1+x)}{2}]e^x$, which obviously satisfies (1). Then we can acquire $\varsigma(x)$ from (1). Fig. 4 shows the exact solution, the numerical solution and the error figure between them. The errors $e(\kappa,\kappa_N)$ for different N are listed in Table 3.

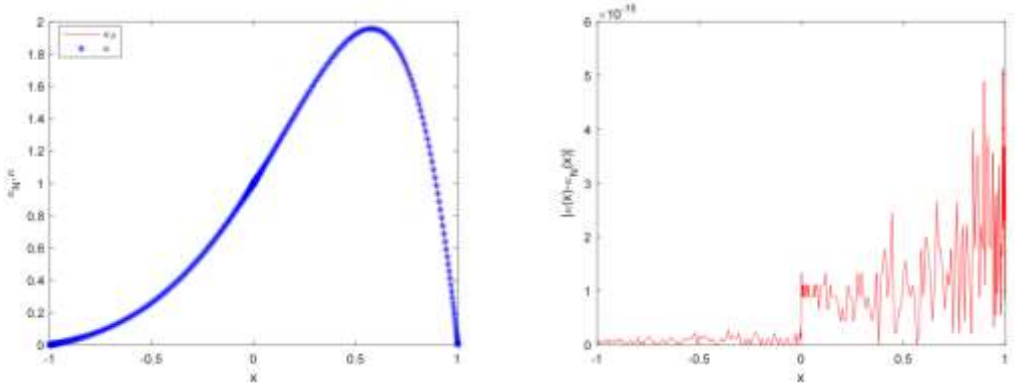

Fig. 4. Figures of the exact solution and the numerical solution with N=60 (left) and the error (right) between them.

TABLE 3. The error between the numerical solution and the exact solution with different N.

	N=20	N=30	N=40
$e(\kappa,\kappa_N)$	1.36557432e-14	5.21804822e-15	3.10862447e-15
	N=50	N=60	N=70
$e(\kappa,\kappa_N)$	1.88737914e-15	1.33226763e-15	1.11022302e-15

Again, we can see from Table 3 that when $N > 30$, the approximate solution has an accuracy of about 10^{-15}. As can be seen from Fig. 4, our algorithm is undoubtedly robust and ultra-high precision.

VI. Concluding Remarks

For one-dimensional second-order interface problem, the existing high-precision algorithms are relatively scarce, and most of them are based on finite element method. Based on this situation, this paper proposes the spectral element method for one-dimensional second-order elliptic interface problem. The error between the approximation solution and the exact solution achieves spectral accuracy and theoretically proves the existence and uniqueness of its solution. This is of practical significance for those interface problems where high dimension can be converted to low dimension. A large number of numerical results show that the proposed algorithm has excellent convergence and accuracy. In addition, it is our future research goal to develop and study high-precision algorithms for interface problems in high dimensions and their equivalent forms in low dimensions.

References

[1] Wang, Q., Liu, J., Gong, C., Tang, X., Fu, G., An efficient parallel algorithm for Caputo fractional reaction-diffusion equation with implicit finite-difference method. Advances in Difference Equations, pp.1-12, 2016.

[2] Chen, L., Shen, J. and Xu, C., A triangular spectral method for the Stokes equations. Numerical Mathematics: Theory, Methods and Applications, 4(2), pp.158-179, 2011.

[3] Lu, Z. and Chen, Y., L∞-error estimates of triangular mixed finite element methods for optimal control problems governed by semilinear elliptic equations. Numerical Analysis and Applications, 2, pp.74-86, 2009.

[4] Bordas, S.P., Burman, E., Larson, M.G. and Olshanskii, M.A. eds., Geometrically unfitted finite element methods and applications: Proceedings of the UCL workshop 2016 (Vol. 121). Springer, 2018.

[5] Li, Z., The immersed interface method using a finite element formulation. Applied Numerical Mathematics, 27(3), pp.253-267, 1998.
[6] Angelova, I.T. and Vulkov, L.G., High-order finite difference schemes for elliptic problems with intersecting interfaces. Applied mathematics and computation, 187(2), pp.824-843, 2007.
[7] Hansbo, A. and Hansbo, P., An unfitted finite element method, based on Nitsche's method, for elliptic interface problems. Computer methods in applied mechanics and engineering, 191(47-48), pp.5537-5552, 2002.
[8] Chen, L., Shen, J. and Xu, C., A triangular spectral method for the Stokes equations. Numerical Mathematics: Theory, Methods and Applications, 4(2), pp.158-179, 2011.
[9] Li, H., A posteriori error estimates for the weak Galerkin finite element methods on polytopal meshes. Communications in Computational Physics, 26(2), 2019.
[10] Shen, J., Stable and efficient spectral methods in unbounded domains using Laguerre functions. SIAM Journal on Numerical Analysis, 38(4), pp.1113-1133, 2000.
[11] Tang, T., Spectral and high-order methods with applications. Beijing: Science Press, 2006.